Domain Structures in Magnetoresistive Granular Metals

A. Gavrin and M. H. Kelley

Electron Physics Group, National Institute of Standards and Technology

Gaithersburg, MD 20899

John Q. Xiao and C. L. Chien

Dept. of Physics and Astronomy, The Johns Hopkins University, Baltimore, MD 21218

We have imaged the magnetic domain structure of several heterogeneous Co_xAg_{1-x} alloys by using scanning electron microscopy with polarization analysis (SEMPA). These images show that extended domain structures exist in both the as-deposited samples and in samples annealed at moderate temperatures. This suggests that a significant fraction of the cobalt in these materials does not contribute to the giant magnetoresistance (GMR). Only those samples annealed at 600 °C and containing less than 40% cobalt by volume show no domain structure.

Recently, several groups have shown that certain granular ferromagnets[1] exhibit giant magnetoresistances (GMR)[2] comparable to those observed in multilayered materials.[3] Such granular ferromagnets are produced by co-sputtering two metals which are immiscible, and of which one is ferromagnetic, e.g., Ag and Co. The resulting material may contain three phases, pure cobalt, pure silver, and a metastable Co-Ag alloy which may be ferromagnetic. High substrate temperature and post-deposition annealing favor segregation of the alloy. The Co-Ag system exhibits large magnetoresistances in the as-deposited state, which suggests that isolated magnetic particles are present.

By using scanning electron microscopy with polarization analysis (SEMPA)[4] to image the magnetic structure, we provide a detailed view of the demagnetized state in several heterogenous Co_xAg_{1-x} alloys (x designates the volume fraction). Our magnetic images show that large magnetic domains exist in these materials over a broad range of compositions and annealing temperatures. These domains are typically 300–600 nm in extent, far larger than the particle size. Such domains can arise under two circumstances: ferromagnetic behavior in the alloy matrix, or long range magnetic correlations among many individual cobalt particles. We will discuss these two mechanisms and their ramifications for understanding GMR in granular materials.

The materials described in this Letter were produced by dc magnetron sputtering onto room temperature Si (100) substrates; the films are several μm thick. The details of this procedure have been discussed elsewhere.[2] The samples cover the composition range $0.35 \leq x \leq 0.50$ in increments of 0.05, and were vacuum annealed at temperatures T_A = 300, 450, and 600 °C. The

compositions of the samples are known to ± 0.005, and the annealing temperatures to ± 25 °C.[5] The magnetoresistance measurements were made using a standard four-probe method with the magnetic field in the film plane and parallel to the current ($\rho_{\parallel}$); we display the data in the form $\Delta\rho/\rho = [\rho(H) - \rho(0)]/\rho(0)$. In Fig. 1, we show room temperature and 5 K magnetoresistance scans of the as-deposited sample with composition $Co_{0.35}Ag_{0.65}$.

The magnetic images were acquired by using scanning electron microscopy with polarization analysis (SEMPA). Because SEMPA is sensitive to only the first few monolayers of material, the sample surface is cleaned prior to measurement by sputtering with Ar^+ ions at 1.15 keV. Examples of SEMPA images are shown in Figs. 2 and 3. The low magnification image shown in Fig. 2 provides an overall view of the domain sizes and shapes. Fig. 3, which was obtained at higher magnification, provides detailed information about the direction of the magnetization within a few domains. Figs. 2a and b show the x and y components of the magnetization respectively. For instance, in Fig. 2a the grey scale represents M to the left (black) through M to the right (white). We calculate the direction of the magnetization from the two component images; Fig. 2c shows the results of that calculation. The inset illustrates the correspondence between color and angle.

The sample imaged here is the same as that referred to in Fig. 1, and the scale is indicated in each of the images. The topographic images (not shown) are almost featureless. The individual cobalt particles are approximately 2–3 nm in diameter,[6] and cannot be resolved with this instrument.[7] Scanning Auger microscopy (SAM) maps of the sample surface show a uniform

distribution of both cobalt and silver down to the resolution limit of the microscope;[7] thus the observed domain structure does not reflect an underlying chemical heterogeneity.

The magnetic structures of all of the as-deposited materials in the composition range $0.35 \leq x \leq 0.50$ are similar in appearance. Thus we will focus on the material with $x = 0.35$. The typical domain size is approximately 300-600 nm. Since the magnetizations are not parallel to the directions of elongation, some of the magnetic flux is being "sourced" or "drained" along the long domain boundaries. Because we only measure the in-plane components of magnetization, we cannot determine whether these divergences reflect a change in the magnitude of the magnetization, or an out-of-plane component.

This is even more apparent in Fig. 3, in which we use a vector map to represent the in-plane surface magnetization field. Several magnetic singularities are evident in this image. For instance, there is a drain near the left edge of the image, with a source just to the right and slightly below; the heavy arrows mark these features. It is possible that this pattern represents the closure domains capping a domain structure which is perpendicular or canted with respect to the film plane. Such domains have previously been observed in amorphous alloys by using Kerr effect microscopy.[8] It is also important to note that the magnetic structures seen in this image are the smallest structures present down to the resolution limit of our instrument.[7]

As noted previously, the magnetization patterns shown in Figs. 2 and 3 are similar to those observed in the samples with $x = 0.40$, 0.45, and 0.50. Furthermore, the patterns are unaffected

by annealing at temperatures of 300 and 450 °C. However, annealing at 600 °C dramatically affects the magnetization patterns. After this treatment, no domains are visible in the sample with $x = 0.35$, and domains are only faintly visible in the sample with $x = 0.40$. For the samples with $x = 0.45$ and above, the domains are clearly visible and somewhat larger than in the unannealed samples. A detailed investigation of the domain morphology will be presented elsewhere.[9] The 600 °C anneal also results in substantial segregation of silver towards the surface of the film, as indicated by Auger depth profiling. Thus, the domain structures observed in the annealed samples may reflect a deficit of cobalt compared to as-deposited samples of the same nominal composition.

We now consider how these domain structures may coexist with giant magnetoresistance. It is widely accepted[10] that the GMR effect results from electron scattering by the moments of isolated magnetic particles. In the demagnetized state, the moments of the cobalt particles are randomly oriented; applying an external magnetic field aligns the magnetizations of the individual particles, reducing the magnetic disorder and thus the scattering. For this mechanism to result in GMR, it is essential that the length scale of the magnetic disorder be less than the relevant scattering length, i.e., the electron mean free path or the spin diffusion length. However, the domains shown in Figs. 2 and 3 have typical dimensions of 300–600 nm, far larger than the either of these.[11] Thus, the GMR must result from cobalt particles which do not participate in the observed domain structure.

As noted earlier in this Letter, it is possible that all of the cobalt particles are uncorrelated in the

demagnetized state, but the Co-Ag alloy matrix retains sufficient cobalt to be ferromagnetic. In that case, the domains which we observe are due entirely to cobalt in the alloy matrix material, and the GMR is due to cobalt which has precipitated out. At zero applied field, the magnetic scattering is due to cobalt particles which are not aligned with one another, or with the ferromagnetic medium in which they are embedded. Only this fraction of the cobalt in the sample participates in the GMR. We would also like to note that Stearns and Cheng discussed the possibility of a ferromagnetic matrix phase in an analysis of their magnetoresistance data.[12]

We can estimate an upper limit on the fraction of the cobalt which gives rise to the GMR. Enough of the cobalt must remain in the alloy matrix to meet two criteria: the matrix must be ferromagnetic at room temperature, and the matrix must percolate throughout the sample. We shall refer to the atomic fraction of cobalt in the matrix as α, and the volume fraction of the sample occupied by the alloy matrix as y.

The threshold for site percolation on an fcc lattice is approximately 0.20 in three dimensions.[13] This sets a lower limit on α at which the Curie temperature of the alloy matrix drops to zero. For a T_c above room temperature, we estimate a minimum value of $\alpha_{min} = 0.30$ on the basis of magnetic phase diagrams for several related systems.[14] Furthermore, if we are to observe large domains due to ferromagnetism in the alloy phase, y must be large enough for that phase to percolate throughout the material. Two reasonable guesses for y are the percolation thresholds for random close packing ($y_{rcp} \approx 0.27$)[12] and for percolation in a granular metal ($y_{granular} \approx 0.55$).[1]

For the sample with $x = 0.35$, restricting $\alpha = 0.30$ and $y = 0.27$, we find the maximum volume fraction of cobalt present in the form of particles to be $x_{max} \leq 0.29 \pm 0.01$. Applying the more stringent condition $y = 0.55$ gives $x_{max} \leq 0.22 \pm 0.01$. It is important to note that this result applies to all samples in which we observe extended domains. Since this includes the samples annealed at 450 °C, we may assume that an even smaller fraction of the cobalt contributes to the GMR in the as-deposited samples. The absence of domains in the $x = 0.35$, $T_A = 600$ °C sample can also be understood. In this sample, the annealing has depleted the alloy matrix of cobalt, thus, ferromagnetism can no longer be sustained.

It is also possible that most of the matrix is nonmagnetic, and the observed domains represent magnetic correlations among many of the isolated cobalt particles. Secondary electrons are emitted from both the matrix and the particle phases, so either can contribute to the observed domain pattern. In this case, the GMR results only from that fraction of the cobalt particles which do not take part in the correlations. Such correlations could be mediated by exchange interactions which we expect to be ferromagnetic for small particle separations.[15] Dipolar interactions are also present, but contribute both ferromagnetic and antiferromagnetic couplings. Because the form of the net interactions among the particles is not known, we may not place a strict limit on the fraction of cobalt particles participating in the correlations. However, we may understand the behavior of the $x = 0.35$, $T_A = 600$ °C sample as follows.

The exchange interaction is proportional to the surface area of the particles, whereas the particle moment varies with its volume. Thus, the effective exchange field ($H_{exch.} = AJ_{exch.}/M_sV$) scales

inversely with the particle size. Furthermore, the exchange constant is expected to decrease as the interparticle separation increases.[14] Since annealing increases both the separation and the mean particle radius, we may expect exchange interactions to be rapidly suppressed by annealing. The two possibilities discussed above are not mutually exclusive: they represent the extreme points on a range of possibilities. That is, it is possible that both the matrix and a fraction of the cobalt particles contribute to the observed domain structure.

We have shown that heterogeneous Co-Ag alloys have a magnetic domain structure at length scales far exceeding those defined by the cobalt particle size and the length scales relevant to electron scattering. This result implies that some or perhaps most of the cobalt does not contribute to the GMR.

This work was supported by NSF Grant No. DMR-9200280 and ONR Grant No. N00014-91-J-1633 at Johns Hopkins, and by the Technology Administration of the U. S. Department of Commerce and the Office of Naval Research for work at NIST. One of us (A. Gavrin) wishes to thank the National Research Council for an Associateship.

FIGURE CAPTIONS

Fig. 1 The magnetoresistance of granular $Co_{0.35}Ag_{0.65}$ as a function of the applied field at temperatures T = 300 K and T = 5 K.

Fig. 2 Images of $Co_{0.35}Ag_{0.65}$ recorded by SEMPA. (a) x component of the magnetization, (b) y component of the magnetization, (c) map of the magnetization direction, with color wheel inset to show direction.

Fig. 3 Arrow map of the magnetization in $Co_{0.35}Ag_{0.65}$ as recorded by SEMPA.

1. B. Abeles, in *Applied Solid State Science: Advances in Materials and Device Research*, edited by R. Wolfe (Academic, New York, 1976), p. 1; C. L. Chien, J. Appl. Phys **69**, 5267 (1991).

2. A. E. Berkowitz, J. R. Mitchell, M. J. Carey, A. P. Young, S. Zhang, F. E. Spada, F. T. Parker, A. Hutten, and G. Thomas, Phys. Rev. Lett. **68**, 3745 (1993); J. Q. Xiao, J. S. Jiang, and C. L. Chien, Phys. Rev. Lett. **68**, 3749 (1993).

3. M. N. Baibich, J. M. Broto, A. Fert, F. Nguyen van Dau, F. Petroff, P. Etienne, G. Creuzet, A. Freidrich, and J. Chazelas, Phys. Rev. Lett. **61**, 2472 (1988); S. S. P. Parkin, N. More, and K. P. Roche, Phys. Rev. Lett. **64**, 2304 (1990).

4. M. R. Scheinfein, J. Unguris, M. H. Kelley, D. T. Pierce, and R. J. Celotta, Rev. Sci. Instrum. **61**, 2501 (1990).

5. Error estimates quoted in this paper are to be interpreted as one standard deviation combined random and systematic errors unless otherwise indicated.

6. P. Xiong, G. Xiao, J. Q. Wang, J. Q. Xiao, J. S. Jiang, and C. L. Chien, Phys. Rev. Lett. **69**, 3220 (1992).

7. The resolution of the microscope has not been measured directly. Furthermore, the resolution is expected to differ among the three operating modes: secondary electron imaging, SEMPA, and Auger mapping. Under the operating conditions used during this investigation, the narrowest features which we have observed to date are as follows. In secondary imaging mode: 25±3 nm (the edge of a cleaved Si wafer). In Auger mode: 45±3 nm (the edge of a lithographically produced structure). In SEMPA mode: 45±3 nm (a domain wall in a Co-Ni hard disk medium).

8. A. P. Malozemoff, W. Fernengel, and A. Brunsch, J. Magn. Magn. Mater. **12**, 201 (1979); G. Dietz and T. Frechen, IEEE Trans. Mag. **MAG-20**, 1858 (1984).

9. A. Gavrin, et al., in preparation.

10. S. Zhang, Appl. Phys. Lett. **61**, 1855 (1992); S. Zhang and P. M. Levy, J. Appl. Phys. **73**, 5315 (1993); T. Valet and A. Fert, J. Magn. Magn. Mater **121**, 378 (1993).

11. Q. Yang, P. Holody, S.-F. Lee, L. L. Henry, R. Loloee, P. A. Schroeder, W. P. Pratt, Jr., and J. Bass, Phys. Rev. Lett. **72**, 3274 (1994).

12. M. B. Stearns and Y. Cheng, J. Appl. Phys. **75**, 6894 (1994).

13. R. Zallen, *The Physics of Amorphous Solids* (John Wiley, New York, 1983), p. 170.

14. C. L. Chien, S. H. Liou, D. Koufalt, W. Yu, T. Egami, and T. R. McGuire, Phys. Rev. B **33**, 3247 (1986); J. R. Childress and C. L. Chien, Phys. Rev. B **43**, 8089 (1991).

15. Z. Celinski, B. Heinrich, and J. F. Cochran, J. Appl. Phys. **73**, 5966 (1993).

FIGURE 1

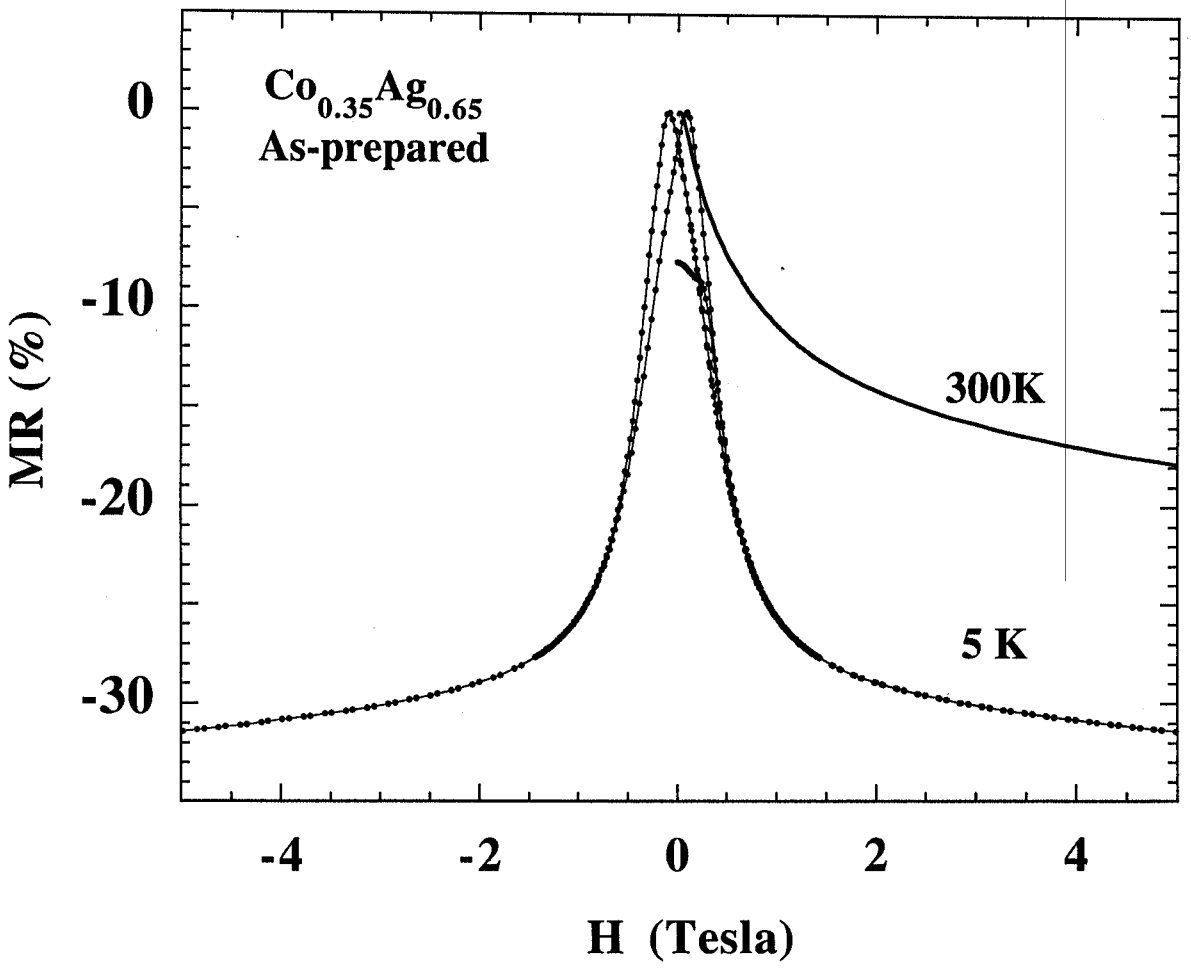

Fig. 2

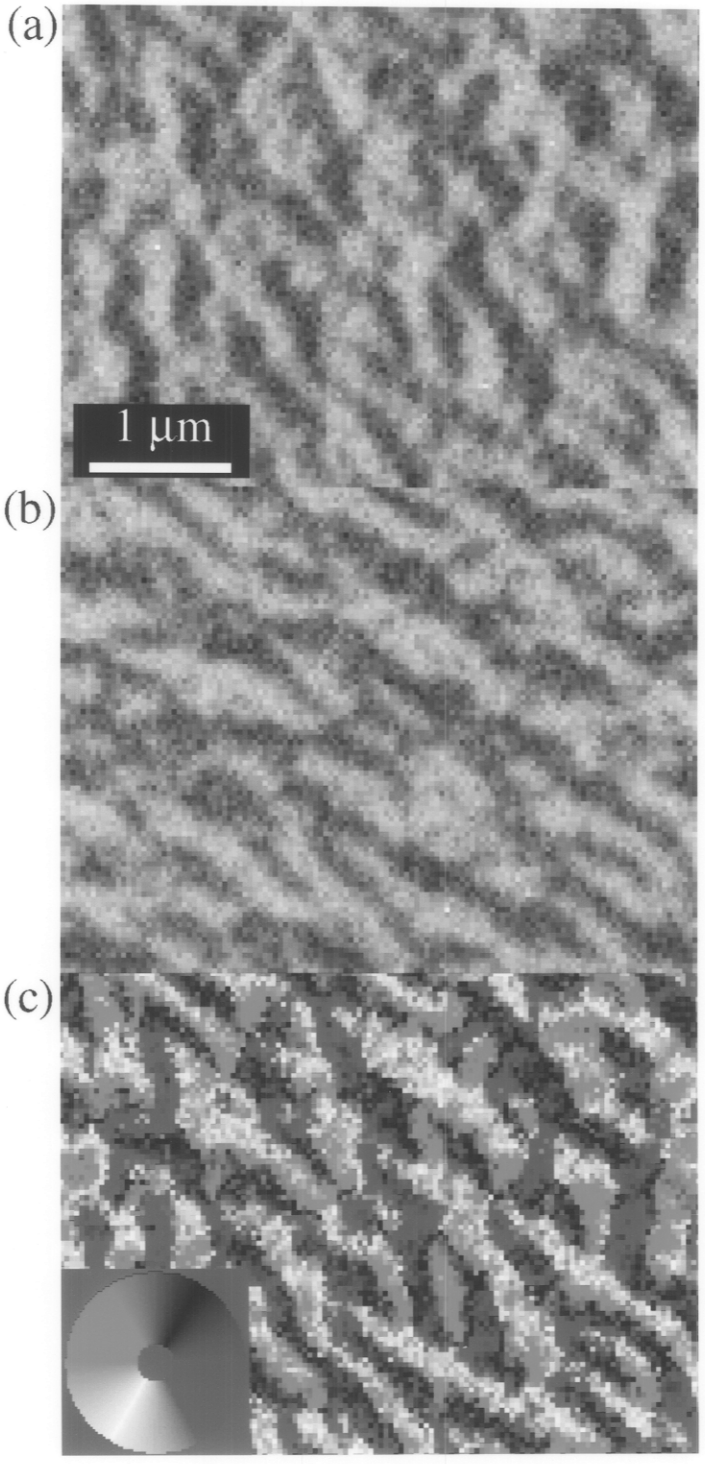

FIGURE 3